Soft Matter

Accepted Manuscript

ROYAL SOCIETY OF CHEMISTRY

www.rsc.org/softmatter

ARTICLE TYPE www. rsc.org/xxxxxx | XXXXXXXX

Commensurability-driven structural defects in double emulsions produced with two-step microfluidic techniques†

Alexandre Schmit,[a] Louis Salkin,[a] Laurent Courbin,[a‡] and Pascal Panizza[a§]

Received Xth XXXXXXXXXX 20XX, Accepted Xth XXXXXXXXX 20XX
First published on the web Xth XXXXXXXXXX 200X
DOI: 10.1039/b000000x

The combination of two drop makers such as flow focusing geometries or ⊤ junctions is commonly used in microfluidics to fabricate monodisperse double emulsions and novel fluid-based materials. Here we investigate the physics of the encapsulation of small droplets inside large drops that is at the core of such processes. The number of droplets per drop studied over time for large sequences of consecutive drops reveals that the dynamics of these systems are complex: we find a succession of well-defined elementary patterns and defects. We present a simple model based on a discrete approach that predicts the nature of these patterns and their non-trivial scheme of arrangement in a sequence as a function of the ratio of the two timescales of the problem, the production times of droplets and drops. Experiments validate our model as they concur very well with predictions.

1 Introduction

Double emulsions, that is, metastable liquid dispersions made of *small droplets* encapsulated inside *large drops*,[1] are used in a variety of industrial applications, e.g. they serve as capsules for drugs[2] or nutrients[3] and microreactors for chemical reactions.[4] In the food industry, applications include their use for the controlled release of flavor or aroma,[5] the production of low-fat food products,[6] and the protection of sensitive food agents.[7] In material science, they are useful templates to fabricate materials as diverse as monodisperse vesicles,[8] polymersomes,[9] liquid crystal shells,[10] microcapsules,[11] and Janus particles.[12] Double emulsions are also promising candidates in biology for cellular reconstitution.[13] For instance, alginate microcapsules can be employed as three-dimensional cellular assays to study the mechanics of tumor progression in vitro.[14] All these applications require an accurate control of the sizes and internal structure (number of encapsulated droplets) as these features monitor the transport kinetics and loading levels of encapsulated species as well as the stability[15] and rheology[16] of double emulsions. In contrast to top-down emulsification methods[1] for which large quantities of fluids are handled at one time, microfluidic technologies allow one to manipulate fluid elements one by one so that periodic trains of highly monodisperse dispersions can be produced[17] and employed to create double emulsions. This bottom-up approach offers unprecedented ways to create double, triple, and even higher-order emulsions with a control over the sizes and number of encapsulated droplets that is expected to be unparalleled.[18–22] In particular, the use of regularly-spaced trains of droplets helps in making the probability distributions of the encapsulated number of droplets per drop narrower than those obtained with other methods limited to random loading characterized by Poisson statistics.[23–25] Finding strategies to control encapsulation processes[25] is particularly important in biology for which applications often require to encapsulate a single cell per drop, random loading techniques yielding in this case more empty and unusable drops than loaded ones. Yet, an understanding of the nature of the defects in the internal structure of double emulsions generated with microfluidics has remained elusive.

Here we introduce a discrete model for the description of the two-step formation of double emulsions in microfluidics. Studying the number of encapsulated droplets per drop over large sequences of consecutive drops, we uncover complex dynamics characterized by a succession of well-defined elementary patterns separated by defects that are intrinsic to these systems. Our model predicts the nature of the patterns and defects as well as their occurrence in a sequence of drops as a function of the ratio of production periods of droplets and drops. We provide experimental results which are well-described by these predictions. Interestingly, this out-of-equilibrium problem that results from the competition between two timescales is analog to commensurate-incommensurate transitions observed in host-guest systems built up from two interpenetrating lattices.[26]

† Electronic Supplementary Information (ESI) available: A supplementary movie to illustrate the presence of defects in the internal structure of double emulsions and a single-page document to provide the derivation some of the properties of sequences of drops and patterns. See DOI: 10.1039/b000000x/

[a] *IPR, UMR CNRS 6251, Campus Beaulieu, Université Rennes 1, 35042 Rennes, France. Fax: 33 2 23 23 67 17; Tel: 33 2 23 23 30 27*
‡ E-mail: laurent.courbin@univ-rennes1.fr
§ E-mail: pascal.panizza@univ-rennes1.fr

2 A discrete model

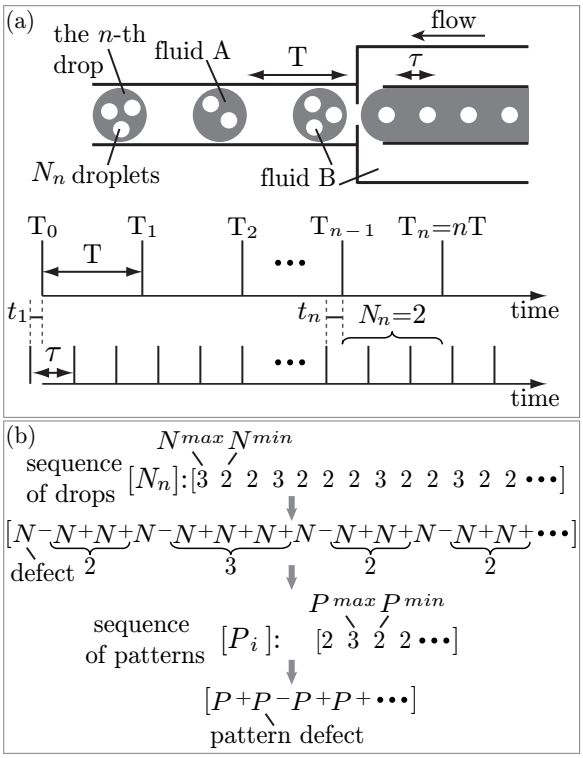

Fig. 1 (a) Schematic of the modeled two-step formation of B-in-A-in-B double emulsions defining the variables at play. (b) Outcomes of the model for a typical sequence of drops.

The first step of the standard dripping technique employed to produce double emulsions consists in generating a periodic train of monodisperse droplets (production period τ) with a droplet maker such as a T junction[27] or a flow focusing geometry.[17] The train is then directed toward a second drop maker producing periodically large monodisperse drops (production period T) [see Fig. 1(a)]. Each of these drops may encapsulate droplets which creates a double emulsion over time. We use a discrete approach to model the encapsulation dynamics over sequences of consecutive drops. The time of the pinch-off of the n-th drop from the nozzle is T_n=nT and we define the time $\tau-t_1$ elapsed between the arrival at the tip of the nozzle of the first droplet and the creation of the first drop [see Fig. 1(a)]; $t_1<$T so that the first drop encapsulates at least one droplet. Building on the description of droplet traffic in microfluidic networks,[28] we neglect the physical volume of the drops. We investigate the case T$>\tau$ so that all drops contain at least one droplet. Then, one straightforwardly derives the following set of two recursive equations that fully describe the encapsulation dynamics as they predict N_n the number of droplets contained in the n-th drop of a sequence:

$$N_n = \text{floor}\,(\text{T}/\tau - 1 + X_n) + 1, \quad (1a)$$
$$X_{n+1} = X_n + \text{T}/\tau - N_n, \quad (1b)$$

where X_n=t_n/τ. X_n corresponds to the time in τ units elapsed between the arrival at the tip of the nozzle of the last droplet encapsulated in the (n-1)-th drop and the time T_{n-1}. Using eqn (1), we predict generic and important properties of the two-step formation of double emulsions (Fig. 1(b) defines the outcomes of the model for a typical sequence $[N_n]$):

(A_1) *Variations in the number of encapsulated droplets per drop do not exceed one unity* as N_n can take only two values: N^{max}=ceil $\left(\overline{N}\right)$ or N^{min}=floor $\left(\overline{N}\right)$.

(A_2) $\overline{N}=\frac{\text{T}}{\tau}$ *is the mean number of droplets per drop*. Indeed, $\overline{N}=\lim_{n\to\infty}\frac{1}{n}\sum_{k=1}^{n}N_k$ and one can easily show that $\sum_{k=1}^{n}N_k\tau=nT+\tau(X_1-X_{n+1})$.

(A_3) $\left|\frac{\text{T}}{\tau}-\text{round}\left(\frac{\text{T}}{\tau}\right)\right|=\mathcal{F}(N^-)$ *is the fraction of defects, i.e. the drops denoted N^- containing the less repeated number of droplets in a sequence*. Conversely, N^+=round$(\overline{N})$ denotes the variable N^{min} or N^{max} appearing the more often in a sequence [see Fig. 1(b)]. This property is a direct consequence of items (A_1)–(A_2).

In general, τ is not a multiple of T so that fluctuations of the number of droplets are bound to occur in a sequence of drops. Considering this general case, we next focus on the properties of defects, discussing their occurrence and the distances between two defects:

(A_4) *Defects are isolated events that dot not appear consecutively in a sequence of drops*. Assuming that N_n=N^-, we demonstrate below that N_{n+1}=N^+. We begin by defining $-\frac{1}{2}<\varepsilon=\overline{N}-N^+<\frac{1}{2}$ and we consider the case $\varepsilon>0$, i.e. N^+=N^{min} and N^-=N^{max}. Using eqn (1), one can show that $1-\varepsilon\leq X_n$ and X_{n+1}=$X_n-1+\varepsilon$. Using these two results, one finds N_{n+1}=floor$(N^+ + 2(\varepsilon-1)+X_n)+1$ and consequently N_{n+1}=N^+ since $2(\varepsilon-1)+X_n<0$; note that a similar demonstration can be derived when $\varepsilon<0$. This result implies that the sequence $[N_n]$ consists of a succession of one or several consecutive N^+ separated by isolated N^-.

We next process the signal $[N_n]$ into a series of patterns $[P_i]$, a pattern being the distance between two defects, i.e. the number of N^+ between two consecutive N^- [see Fig.1(b)]. As shown below, such an analysis of the response helps to determine the conditions for the emergence of periodicity in the occurrence of defects. N_{cyc} and N_{pat} being respectively the number of drops and patterns per cycle, the number of N^- per cycle corresponds to N_{pat} [see (A_4)] so that $\mathcal{F}(N^-)=\frac{N_{pat}}{N_{cyc}}$. Using ($A_1$)–($A_3$), it is straightforward to show that $\overline{N}=N^+ + \frac{N_{pat}}{N_{cyc}}(N^- - N^+)$ for any ε. Since N_{cyc} and N_{pat} are natural numbers, $\overline{N}=\frac{\text{T}}{\tau}$ being a rational number is a necessary condition for periodicity so that:

(A_5) *The system necessarily exhibits aperiodicity whenever* τ *and* T *are incommensurate.*

As demonstrated below, the necessary condition turns out to be a sufficient one, hence:

(A_6) *When* τ *and* T *are commensurate, the dynamics of the system are periodic.*

For the sake of simplicity, we next provide a demonstration of sufficiency in the case N^+=N^{min} and N^-=N^{max} (ε>0). We begin by indexing a sequence with N_1=N^- and we define k_i, the index of the (i+1)-th N^- found in $[N_n]$. Using eqn (1), we show that X_k=$X_1+(k-1)\varepsilon-1$ when $1<k<k_1$ as X_2=$X_1+\varepsilon-1$ and N_k=N^+. Since N_{k_1}=N^-, using eqn (1b) and the relationship established above one finds k_1=ceil($\frac{1}{\varepsilon}$) + 1. With a similar approach and a recursive method, one then obtains k_i=ceil($\frac{i}{\varepsilon}$) + 1 and X_{k_i}=$X_1+(k_i-1)\varepsilon-(i-1)$. When τ and T are commensurate, we can express ε as the irreducible fraction $\frac{p}{q}$, p and q being two integers. Using this expression of ε and the two relationships derived previously, one easily shows that the dynamics of the system are periodic since k_p=q and X_{k_p}=X_1. Consequently, q and p respectively are N_{cyc} and N_{pat}.

Similarly to the predicted features of the sequences $[N_n]$, our model predicts four properties for the sequences of patterns $[P_i]$ (we provide their derivations in the ESI†):

(A_7) *Variations in the number of drops per pattern do not exceed one unity* since P_i can take only two values: P^{min}=floor $\left(\frac{1}{|\varepsilon|}\right)-1$ and P^{max}=ceil $\left(\frac{1}{|\varepsilon|}\right)-1$.

(A_8) $\overline{P}$=$\frac{1}{|\varepsilon|}-1$ *is the mean number of drops per pattern.*

(A_9) $\left|\frac{1}{|\varepsilon|}-\text{round}\left(\frac{1}{|\varepsilon|}\right)\right|$=$\mathcal{F}(P^-)$ *is the fraction of the pattern defects, i.e. the patterns denoted* P^- *containing the less repeated number of* N^+ *in a sequence of patterns. Conversely,* P^+=round($\overline{P}$).

(A_{10}) *Defects are not consecutive in a sequence of patterns.*

The predicted features do not depend on initial conditions, i.e. the time t_1, but are fully described by the value of $\frac{T}{\tau}$. This important property will allow us to validate our model by comparing predictions with experiments for which initial conditions cannot be controlled.

3 Experiments

We use two coaxial drop makers to fabricate oil-in-water-in-oil double emulsions with a two-step formation (see Fig. 2).[29] First, using two syringe pumps, an oil 1 (DC 200, Fluka) and an aqueous phase (a mixture of 90 wt.% glycerol and distilled water) are respectively injected through a needle centered in a cylindrical tube and inside this tube. Periodic trains of monodisperse oil droplets flowing at a constant velocity are then created. Variations of q_1 and q_2, the respective flow rates of oil 1 and aqueous phases, allow for the control of the droplet production period τ and droplet volume Ω_{in}=$q_1\tau$.

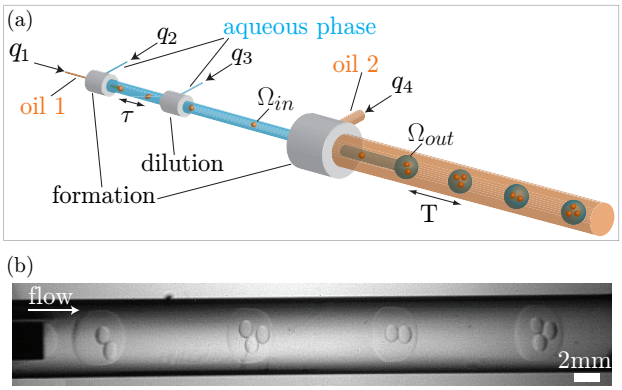

Fig. 2 (Color online) (a) Schematic of the set-up used to create double emulsions defining experimental parameters. (b) Photograph showing that the number of droplets per drop is not constant over time. The parameters are q_1=0.01 mL min^{-1}, q_2=0.1 mL min^{-1}, q_3=−0.02 mL min^{-1} (the minus sign indicates that the aqueous phase is withdrawn), q_4=0.38 mL min^{-1}, τ=3.6 s, and T=9.03 s.

We use a dilution module[30] to either dilute or concentrate the train with an additional injection or withdrawal of the aqueous phase at a constant flow rate q_3 (Fig. 2). The train is then directed towards the second drop maker where, injecting a sunflower oil 2 (Lidl, France) through the maker's tube at a constant flow rate q_4, monodisperse aqueous drops (volume Ω_{out}) are periodically created with a production period T. When these drops form, they may encapsulate one or several oil droplets which create a double emulsion (see Fig. 2(b) and Movie S1 in the ESI†). Images of the flow are recorded with a camera (EO-1312C, Edmund Optics) and processed to determine Ω_{in}, Ω_{out}, τ, T, and N_n over large sequences of consecutive drops. For each set of experiments, q_1 and q_2 are set to obtain a desired value of τ and Ω_{in}. We then adjust T by either varying q_3 or q_4 while maintaining τ, thus Ω_{in}, unchanged. For each experiment, a sequence $[N_n]$ consists of 100 consecutive drops that are analyzed

Figure 3 shows the evolution with N_n of the probability distribution of the number of encapsulated droplets $\mathcal{P}(N_n)$ for different values of T/τ and a given droplet volume Ω_{in}. As predicted in (A_1), experiments show that N_n never varies by more than one unity in a sequence of drops for any ratio T/τ (see Fig. 3). Additionally, when we compare the measured $\mathcal{P}(N_n)$ in our case of regularly-spaced trains of droplets with the probability distribution that would be expected for a random loading process, i.e. $\overline{N}^{N_n}e^{-\overline{N}}/N_n!$, we find that the former is much narrower than the latter (Fig. 3). Microfluidics indeed offers unique possibilities for droplet ordering that allows one to controllably load discrete fluid elements (e.g. droplets, cells or particles) into drops and to overcome

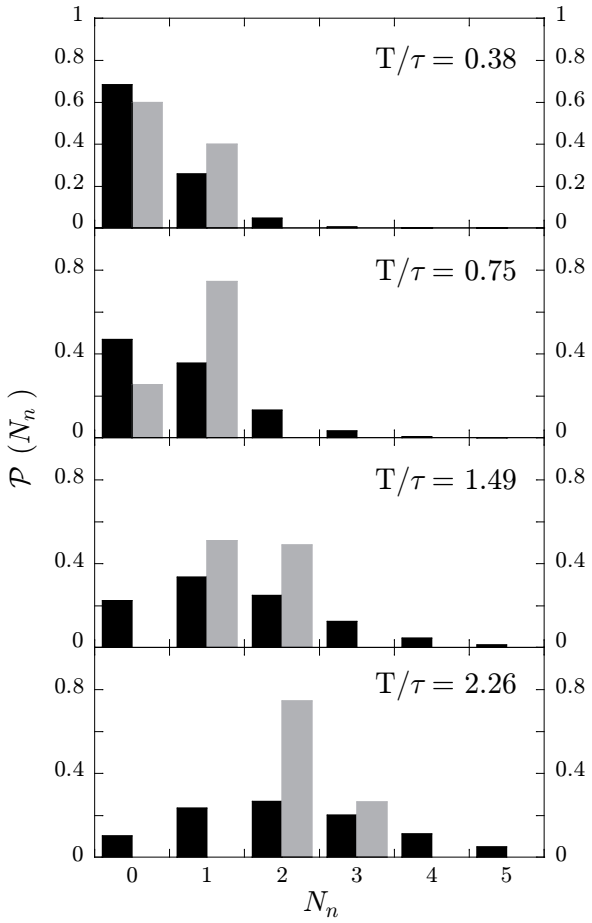

Fig. 3 Experimental probability distributions (grey rectangles) $\mathcal{P}(N_n)$ of the number of droplets per drop measured for Ω_{in}=530 nL and four values of T/τ as shown in the figure. The expected probability distributions (black rectangles) $\mathcal{P}(N_n) = \overline{N}^{N_n} e^{-\overline{N}}/N_n!$ for a random loading process described by Poisson statistics are provided for comparison.

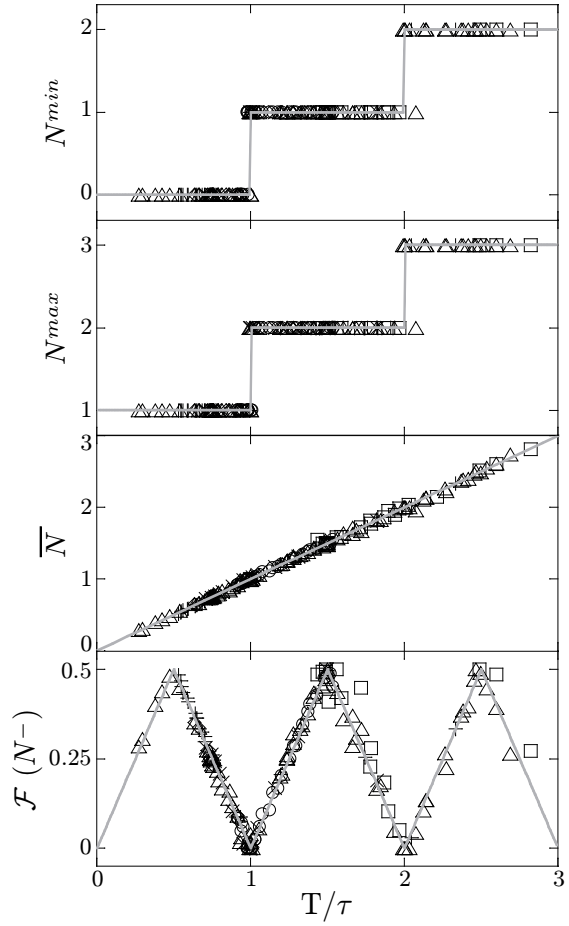

Fig. 4 Experimental variations of N^{min}, N^{max}, $\overline{N}$, and $\mathcal{F}(N^-)$ with $\frac{\mathrm{T}}{\tau}$. The six shapes stand for different values of Ω_{in}=224–565 nL. The continuous lines are predictions that are calculated using the expressions given in items (A_1)–(A_3).

the limitations introduced by Poisson statistics on the loading distributions.[23–25] Performing systematic experiments as a function of T/τ for different droplet volumes Ω_{in}, we find that the measurements of N^{min}, N^{max}, $\overline{N}$, and $\mathcal{F}(N^-)$ mirror the predictions (A_1)–(A_3) (see Fig. 4).

To compare more quantitatively random loading processes and our experiments using regularly-spaced trains of droplets, we report in Fig. 5 the standard deviation σ of $\overline{N}$ for both flow configurations. In our case, using the predicted properties of the sequences $[N_n]$ it is straightforward to show that $\sigma=\sqrt{|\varepsilon|\,(1-|\varepsilon|)}$. As shown in Fig. 5, this predicted standard deviation which concurs well with experimental findings is a periodic function of T/τ that is equal to 0 when $\overline{N} \in \mathbb{N}$ and is always smaller than 0.5. Hence, the standard deviation of $\overline{N}$ for ordered droplets is always smaller than the standard deviation ($\sqrt{\overline{N}}$) that would be obtained in the case of purely random loading (see Fig. 5).

We now compare experimental results with the predicted dynamical properties of the sequences. The predicted period of the system is a non-analytic function of T/τ. Consequently, validating predictions (A_5)–(A_6) is not feasible as it would require to carry out experiments with an infinite number of drops. Nevertheless, we successfully compare below experiments and the predicted properties (A_4) and (A_7)–(A_{10}). As stated in item (A_4), two consecutive N^- never appear in experimental sequences $[N_n]$ and we then process this signal into series of patterns $[P_i]$. Figure 6 shows that the variations of P^{min}, P^{max}, and $\mathcal{F}(P^-)$ with T/τ concur very well with the predictions (A_7)–(A_9). Additionally, experiments show that two P^- are never observed consecutively in a series $[P_i]$

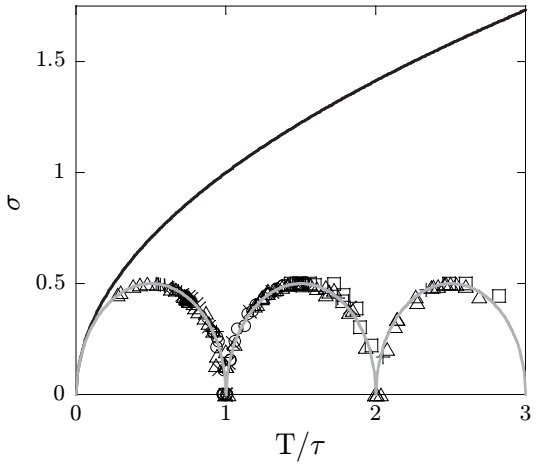

Fig. 5 Variations the standard deviation σ of $\overline{N}$ with $\frac{\mathrm{T}}{\tau}$: the experimental data points whose shapes are identical to those of Fig. 4 are described by $\sigma=\sqrt{|\varepsilon|\,(1-|\varepsilon|)}$ (grey line). The standard deviation in our experiment is compared with that of random loading governed by Poisson statistics, that is, $\sigma=\sqrt{\overline{N}}$ (black line).

as predicted [see (A_{10})]. The evolution of $\mathcal{F}(P^-)$ with T/τ in Fig. 6(a) indicates the non-trivial and complex nature of the response; for better readability, we also provide its variations with $1/|\varepsilon|$ in Fig. 6(b).

4 Conclusions

Introducing a discrete model to describe the two-step formation of double emulsions in microfluidics using periodic trains of droplets, we observe a complex droplet-in-drop encapsulation dynamics characterized by sequences of patterns and defects that are functions of the ratio of the production periods of drops and droplets. Despite its simplicity, our model which neglects the physical volumes of the dispersed fluid elements captures remarkably well both structural and dynamical features of our experiments carried out at constant flow rates for different volumes of droplets.

Our results provide a rationale for the structural defects that are intrinsic to double emulsions produced with microfluidics. The predicted generic properties of the sequences of patterns and defects in these fluid systems should offer robust ways to engineer double emulsions with the standard two-step microfluidic method. The discrete approach used in this work can be easily extended to describe the multi-step formation of more complex fluid systems such as higher-order multiple emulsions and double emulsions having multiple compartments.[31] In addition, it is worthwhile mentioning that for experiments performed at constant pressures, hydrodynamic feedbacks should come into play and result in couplings between the production periods; it is likely that such a situation would require a more complicated theoretical description. Finally, the similarities between this problem and commensurate-incommensurate transitions observed in one-dimensional (1D) systems also illustrate 1D microfluidic arrays of double emulsions as simple mimetic systems of 1D modulated host-guest structures.[26]

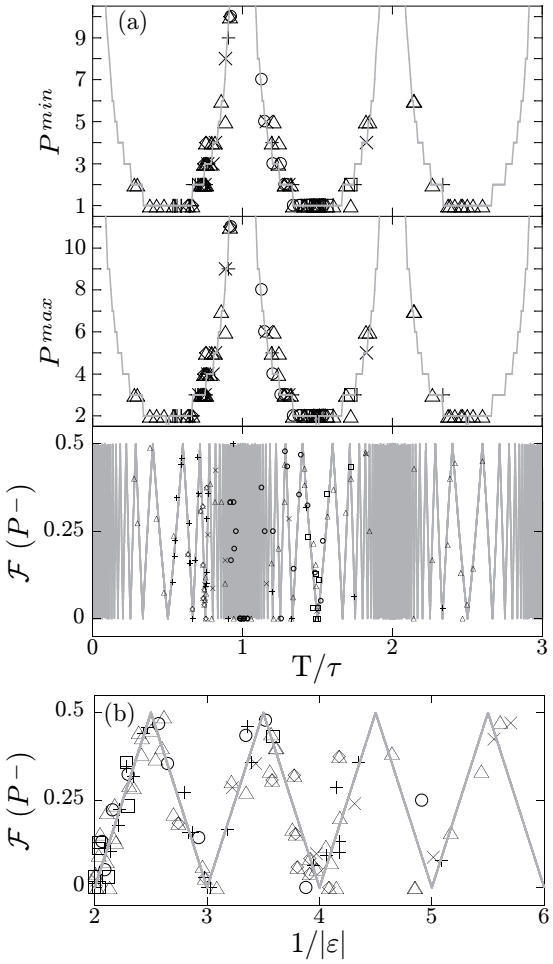

Fig. 6 (a) Variations of P^{min}, P^{max}, and $\mathcal{F}(P^-)$ with $\frac{\mathrm{T}}{\tau}$. (b) Evolution of $\mathcal{F}(P^-)$ with $1/|\varepsilon|$. The lines are predictions of the model. The shapes of the experimental data points are identical to those of Fig. 4.

Acknowledgements

We thank D. Bartolo, N. Pannacci and P. Tabeling for fruitful discussions and C. Lauricella and S. Testu for performing preliminary experiments. We acknowledge partial support from l'Université Européenne de Bretagne (Grant EPT *Physfood*),

le Fonds Européen de Développement Régional (FEDER) and le Conseil Régional de Bretagne.

References

1 F. Leal-Calderon, V. Schmitt and J. Bibette, *Emulsion Science-Basic: Principles*, Springer, New York, 2007.
2 R. Engel, S. J. Riggi and M. J. Fahrenbach, *Nature*, 1968, **219**, 856.
3 G. Muschiolik, *Curr. Opin. Colloid Interface Sci.*, 2007, **12**, 213.
4 H. C. Shum, A. Bandyopadhyay, S. Bose and D. A. Weitz, *Chem. Mater.*, 2009, **21**, 5548.
5 A. G. Gaonkar, 1994, US 5322704.
6 C. Lobato-Calleros, E. Rodriguez, O. Sandoval-Castilla, E. J. Vernon-Carter and J. Alvarez-Ramirez, *Food. Res. Int.*, 2006, **39**, 678.
7 W. Daisuke, I. Noriko, U. Akira and S. Takuya, 2004, JP 2004097113 A.
8 H. C. Shum, D. Lee, I. Yoon, T. Kodger and D. A. Weitz, *Langmuir*, 2008, **24**, 7651.
9 A. Perro, C. Nicolet, J. Angly, S. Lecommandoux, J. F. Le Meins and A. Colin, *Langmuir*, 2011, **27**, 9034.
10 A. Fernández-Nieves, V. Vitelli, A. S. Utada, D. R. Link, M. Márquez, D. R. Nelson and D. A. Weitz, *Phys. Rev. Lett.*, 2007, **99**, 157801.
11 A. S. Utada, E. Lorenceau, D. R. Link, P. D. Kaplan, H. A. Stone and D. A. Weitz, *Science*, 2005, **308**, 537.
12 C. H. Chen, R. K. Shah, A. R. Abate and D. A. Weitz, *Langmuir*, 2009, **25**, 4320.
13 A. P. Liu and D. A. Fletcher, *Nat. Rev. Mol. Cell Bio.*, 2009, **10**, 644.
14 K. Alessandri, B. Ranjan Sarangi, V. Valériévitch Gurchenkov, B. Sinha, T. Reinhold Kießling, L. Fetler, F. Rico, S. Scheuring, C. Lamaze, A. Simon, S. Geraldo, D. Vignjević, H. Doméjean, L. Rolland, A. Funfak, J. Bibette, N. Bremond and P. Nassoy, *Proc. Natl. Acad. Sci. USA*, 2013, **110**, 14843.
15 K. Pays, J. Giermanska-Kahn, B. Pouligny, J. Bibette and F. Leal-Calderon, *Phys. Rev. Lett.*, 2001, **87**, 178304.
16 J. Wang, J. Liu, J. Han and J. Guan, *Phys. Rev. Lett.*, 2013, **110**, 066001.
17 S. L. Anna, N. Bontoux and H. A. Stone, *Appl. Phys. Lett.*, 2003, **82**, 364.
18 S. Okushima, T. Nisisako, T. Torii and T. Higushi, *Langmuir*, 2004, **20**, 9905.
19 L. Y. Chu, A. S. Utada, R. K. Shah, J. W. Kim and D. A. Weitz, *Angew. Chem. Int. Ed.*, 2007, **46**, 8970.
20 N. Pannacci, H. Bruus, D. Bartolo, I. Etchart, T. Lockhart, Y. Hennequin, H. Willaime and P. Tabeling, *Phys. Rev. Lett.*, 2008, **101**, 164502.
21 W. Engl, R. Backov and P. Panizza, *Curr. Opin. Colloid Interface Sci.*, 2008, **13**, 206.
22 W. Wang, R. Xie, X.-J. Ju, T. Luo, L. Liu, D. A. Weitz and L. Y. Chu, *Lab Chip*, 2011, **11**, 1587.
23 M. Chabert and J. L. Viovy, *Proc. Natl. Acad. Sci. U.S.A.*, 2008, **105**, 3191.
24 J. F. Edd, D. D. Carlo, K. J. Humphry, S. Köster, D. Irimia, D. A. Weitz and M. Toner, *Lab Chip*, 2008, **8**, 1262.
25 A. R. Abate, C.-H. Chen, J. J. Agresti, and D. A. Weitz, *Lab Chip*, 2009, **9**, 2628.
26 B. Toudic, P. Garcia, P. Rabiller, C. Ecolivet, E. Collet, P. Bourges, G. J. McIntyre, M. D. Hollingsworth and T. Breczewski, *Science*, 2008, **319**, 69.
27 P. Guillot and A. Colin, *Phys. Rev. E*, 2005, **72**, 066301.
28 D. A. Sessoms, A. Amon, L. Courbin and P. Panizza, *Phys. Rev. Lett.*, 2010, **105**, 154501.
29 P. Panizza, W. Engl, C. Hany and R. Backov, *Colloids Surf. A*, 2008, **312**, 24.
30 M. Belloul, W. Engl, A. Colin, P. Panizza and A. Ajdari, *Phys Rev. Lett.*, 2009, **102**, 194502.
31 A. Schmit, L. Salkin, L. Courbin and P. Panizza, unpublished work.

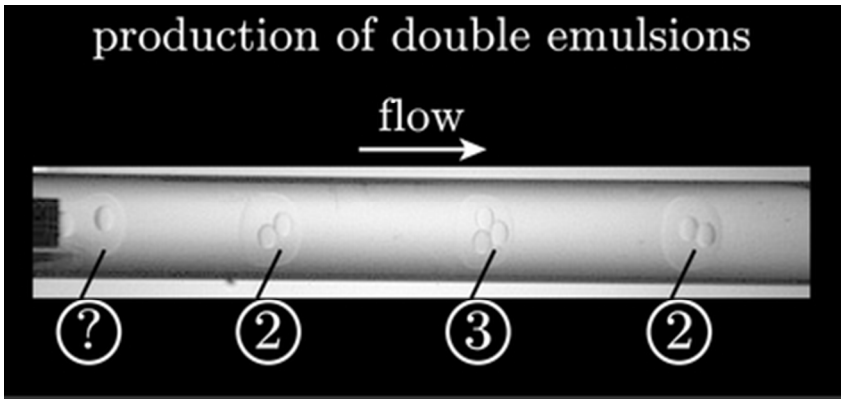

We introduce a model that describes the defects in the internal structure of double emulsions created with two-step microfluidic methods.
35x16mm (300 x 300 DPI)